JOURNAL OF COASTAL AND HYDRAULIC STRUCTURES

Vol. 6, 2026, 56

Laboratory experiments on the propagation of bores induced by offshore soliton forcing over reef flats

Nana Yamaguchi [1], Naoto Inagaki [2], Tomoyuki Takabatake [3], Miguel Esteban [4*], and Tomoya Shibayama [5]

Abstract

This study investigates, in a two-dimensional wave flume, how idealized reef-flat roughness and reef-flat length affect the transformation of solitary-wave-induced bores. Field surveys following natural disasters show that there is some confusion about the degree of protection reef flats can actually offer, and various theories have been put forward. Some researchers claim that coral reefs offer protection from tsunamis, others that they enhance damage to settlement by accelerating the velocity of the wave, and a third group that they neither protect nor exacerbate the damage due to these events. In this study, the authors aim to examine the effect that coral reef analogues have on bores propagating over reef flats by means of laboratory experiments conducted on a two-dimensional wave flume, in order to provide some guidance regarding the effect that idealized reef flats can play on disaster risk mitigation. Forty-eight cases of experiments were tested by using two different water depths, two lengths of reef flat, three types of surfaces (to represent different types of idealized corals), and four different input wave heights into the wave generator. The results indicate that the reduction in both wave heights and wave front velocities was greater in the cases where there were structures representing corals, and for longer reef flats. Also, the attenuation of wave energy was greater with reduced water depth, which in nature usually correlates with a healthy reef system.

Keywords

Solitary waves, reef flat, propagation, laboratory experiments, corals, reef flat roughness

[1] Waseda University, Tokyo, Japan
[2] Kumamoto University, Kumamoto, Japan
[3] Kindai University, Osaka, Japan
[4] Waseda University, Tokyo, Japan
[5] Chuo University, Tokyo, Japan
* esteban.fagan@gmail.com

Research Article. **Submitted:** 25 April 2026. **Reviewed:** 10 June 2026. **Accepted** after double-anonymous review: 25 August 2026. **Published:** 21 September 2026.

DOI: 10.59490/jchs.2026.0056.

Cite as: Yamaguchi, Nana; Inagaki, Naoto; Takabatake, Tomoyuki; Esteban, Miguel; Shibayama, Tomoya (2026): Laboratory experiments on the propagation of bores induced by offshore soliton forcing over reef flats, Journal of Coastal and Hydraulic Structures, 6, https://doi.org/10.59490/jchs.2026.0056

ISSN: 2667-047X online

1 Introduction

Tsunamis can cause devastation to large sections of a coastline, inflicting severe casualties to any inhabited areas that are not well prepared to withstand them. To counteract such events, concrete structures and other types of infrastructure have been built along long sections of shorelines at risk, particularly in the case of Japan. However, building these concrete structures requires substantial financial investment, and thus may not always be economically affordable, particularly for the case of developing countries. After the *2004 Indian Ocean Tsunami*, which killed more than 220,000 persons and caused approximately US $9.9 billion damage from direct impacts (ADPC 2005), much research has been conducted on how coastal environment countermeasures such as mangroves, coral reefs, sand dunes, and sea grasses can offer protection from tsunami events.

Some field surveys reports have indicated how such coastal ecosystems can offer protection from tsunami impacts (e.g. Cochard et al., 2008, Majumdar et al., 2019). While much emphasis has been placed on the study of coastal forests in general, and mangroves in particular (e.g. Alongi, 2008, Kathiresan and Rajendran, 2005, Tanaka et al., 2007) studies on the effect that coral reefs can have on tsunami hydrodynamics are limited and have remained mostly anecdotal, relying mostly on post-disaster field observations following large events.

Coral reefs are large underwater structures composed of the skeletons of colonial marine invertebrates called corals. Each individual coral is referred to as a polyp, which lives on the calcium carbonate exoskeletons of their ancestors, adding their own exoskeleton to the existing structure of the colony. As the years pass the coral reef gradually grows, one tiny exoskeleton at a time, until they become massive structural features of the underground marine environment. Coral reefs are composed of outer and fore reefs, separated by a reef edge. The inner reefs develop from the reef edge to the shoreline, in an area of shallow water generally referred to as the reef flat, while the outer reefs develop on the reef edge (reef slope). Generally speaking, there are three different types of coral reef structures. Fringing reefs form around the shores of land masses and often have a short reef flat. Barrier reefs have a long reef flat that can sometimes be 10–100 km in width, with coral lagoons inside them that can have a water depth of 10–80 meters. Atolls forms in a ring shape inside of coral reefs, generally following the submergence of an extinct volcano (Yamamoto and Esteban, 2014). There is considerable variation within coral species, with branch and bolder forming corals being two of the major types.

Coral reefs appear in tropical seas where the water temperature ranges between 18 to 30 °C. Due to global warming, the risk of mass bleaching events that can kill widespread regions of coral reefs is increasing (Burke et al., 2011). Bleaching occurs when corals expel the symbiotic algae (zooxanthellae) living within them, which provides them their distinctive colour, and turns white. Corals can survive a bleaching event and regain their symbiotic algae, though these episodes of high-water temperature can increase stress to them and result in mass mortality. When they die completely an important element preventing erosion and supplying sediments to the coastline is removed, which can have important consequences in terms of wave hydrodynamics.

In the aftermath of the *2004 Indian Ocean Tsunami* (Shibayama, 2015) and the *2009 Samoan Tsunami* (Mikami 2015), a number of field surveys reports have analysed the effect of coral reefs on tsunami propagation and inundation patterns. However, such field observations have led to a variety of hypothesized theories on the effect that coral reefs can have on tsunami energy dissipation, a process that remains poorly understood. Some researchers mention that coral reefs appear to have offered protection from the incoming tsunami. The surveys conducted in Sri Lanka following the 2004 tsunami mention that areas with less coral reefs experienced higher inundation levels and greater destruction to coastal settlements, as such areas became “low-resistance paths” (Fernando et al., 2011). Reports from the *2009 Samoan Tsunami* noted that residents were able to observe wave breaking on the reefs and that this acted as a trigger to prompt them to evacuate (Shibayama et al., 2010). Also, it was reported that, as the waves broke on top of the reefs, part of the energy of wave was dissipated (Shibayama et al., 2010). However, other researchers indicated that such underwater organic structures did not offer any protection against tsunami inundation. A field survey in Aceh, Indonesia following the 2004 Indian Ocean Tsunami mentioned that healthy reefs did not mitigate the damage to land behind them, but instead that the inundation distance was largely determined by wave height and coastal topography (Baird et al., 2005).

Yet, a third group (e.g. Cochard et al., 2008; Chatenoux and Peduzzi, 2006) mentions that coral reefs might have contributed to accelerating the velocity of tsunami waves, rather than offering any protection. A study on Aceh, Indonesia reports that although under specific condition closed, intact reefs can provide some protection, water may be accelerated through channels in fragmented reefs, causing even greater destruction locally to land behind them (Cochard et al., 2008). Moreover, research which looked into environmental features after the *2004 Indian Ocean Tsunami* mentions that although sea grass offered some protection against the tsunami, coral reefs led to a greater impact on land (Chatenoux and Peduzzi, 2006).

Lowe et al. (2005) measured the wind wave heights and velocities in an actual fore reef and reef flat, which were used to estimate rates of dissipation by wave breaking and bottom friction, concluding that bottom friction dominates the energy dissipation over the reef flat. Lowe et al. (2007) then conducted field experiments on a shallow reef flat using an array of plastic cylinders, measuring the flow inside and above the canopy array, and arrived at the conclusion that wave energy is dissipated at a greater rate amongst the short-period wave components. Buckley et al. (2016, 2018, 2022) conducted experiments and revealed that there is a correlation between the roughness of the surface due to coral reefs and the protection offered against wind waves. Quironga and Cheung (2013) investigated the transmission of solitary waves over fringing reefs, taking into account bed-form form roughness, and found that as roughness increased the solitary waves broke earlier and more energy was dissipated. Fernando et al. (2008) conducted laboratory experiments using solitary waves on the different coverage of coral reefs and confirmed the areas without coral reefs cause local flow intensification. An experiment on the wave propagation mechanism over a reef flat with a pit (placed in the middle of the reef, with a size of 0.8 cm, or 2/9 of the length of the reef flat) conducted by Yao et al. (2020) discovered a correlation between the swell wave height and the pit, as infragravity wave heights near the shoreline are consistently reduced by an average of 10.5% by the pit. Sekimoto et al. (2011) looked at the reef slope and discovered that the wind wave deformation near the reef edge has very strong nonlinearity and results in wave breaking at the reef edge during the uprush, and a hydraulic jump forming at the wave front during the backrush. It is also worth noting that some reef profiles have a "reef crest" that is situated seawards of the "reef flat", and which essentially acts like a submerged detached breakwater. A number of researchers in the past have looked at wave transmission over low-crested structures, including Ahrens (1987), Van der Meer (1990), Hanson and Kraus (1989), or Seabrook et al. (1998), and much is known about how traditional structures (on the shore or offshore) are affected by wind waves (Hofland et al., 2023; Seemann et al., 2023; Sorgatz et al., 2023; van der Meer et al., 2024; van Gent, 2024; Den Bieman et al., 2024)However, while it is clear that some studies have looked at the topography of reefs, little work has been done on how bores propagate over "reef crests" and along "reef flats" of varying lengths, and on how various types of bottom roughness can affect wave hydrodynamics.

Some authors have also conducted numerical simulations to understand the degree of protection that can be offered by reef structures. Mikami and Shibayama (2012) conducted simulations using an LES model and concluded that the wide reef flat plays a role in dissipating tsunami wave energy, with longer reef flats dissipating more energy. Another study conducted by Kunkel et al. (2006) revealed that the broader and shallower the reef is, the more protection it can provide against tsunamis. Moreover, healthy reefs are reported to be more likely to offer protection from tsunamis. A study conducted by Gelfenbaum et al. (2011) also suggested that coral roughness is important in determining the manner in which a fringing reef affects tsunami inundation (which is something that has also been investigated for mitigating wave energy dissipation in general; Villanoy et al., (2012), using a SWAN model, also mention that healthy reefs are effective for mitigating high energy wave impact, since they offer rougher surfaces compared to dead coral -which are much smoother-). However, to date no comparative study has been conducted on how different types of coral colonies – represented by different surface roughnesses- and reef lengths might affect solitary wave hydrodynamics in a flume experiments. It is important to try to further understand how coral reef can protect against tsunamis, given the devastating effects they can have along coastlines around the world (Esteban et al., 2021), and that there is some concern that their heights might be influenced in the future by non-linear effects due to sea level-rise (making the study of how they are affected by coral reefs particularly relevant).

The aim of the present study will thus be to investigate, under controlled flume conditions, how reef-flat length and idealized bed roughness (to model different types of idealized coral environments) will affect solitary-wave breaking, bore formation, and bore attenuation over reef-flat analogues. In doing so, the study intends to clarify hydrodynamic processes rather than reproduce tsunami-scale conditions directly, which can provide some degree of physical understanding of whether the simulations of Mikami and Shibayama (2012), and Kunkel et al. (2006) provide an accurate description of the wave hydrodynamics that could be expected. Given the heterogeneous nature of reefs, particular attention will be paid to how different coral morphologies (represented in the experiments by changes in rugosity) affect solitary wave patterns, and how different lengths affect wave hydrodynamic processes.

2 Experimental program

Laboratory experiments were conducted from November to December 2021 using solitary waves generated by a wave paddle in a wave flume (dimensions 14 m x 0.4 x 0.8 m) at Waseda University, Tokyo, Japan. The computer-controlled piston-type paddle was designed specifically to generate solitary waves, with the speed and location of the paddle being calculated using solitary wave theory. The experimental layout that was employed is shown in Figure 1. Froude scaling of 1:100 was employed.

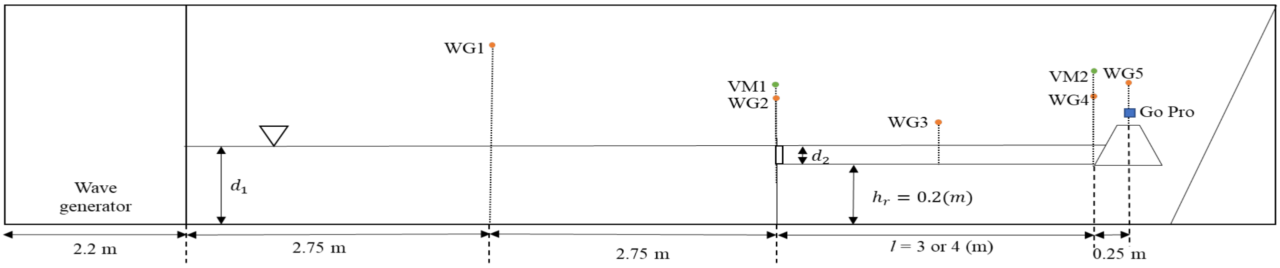

Figure 1: Experimental layout (not to scale).

A metal false bed, acrylic panels, and corrugated plastic were used to construct the experimental layout (see Figure 1), which represented a reef flat and the reef edge. Also, a wood piece 3 cm in height and 2 cm in width was placed at the edge of the reef flat, to represent the reef crest (see Figure 2). The horizontal section of the acrylic panels on top of the metal false bed (representing the reef flat section) were placed 5.5 m away from the wave generator, to a level of 0.2 m above the flume bed (i.e., h_r in Figure 1 was set to be 0.2 m). Two different conditions were used for the length of the reef flat, either 3 m or 4 m. At the end of the horizontal section, another metal false bed with a slope of 1:2 was placed to represent the beach. The experimental cases were repeated for three different conditions of the surface of the reef flat. The first case was a smooth surface with only acrylic panels (which had a thickness of 0.5 cm) placed onto the metal bed. For the second case, a polyethylene layer was fixed on top of the acrylic panel, which was chosen to mimic a branching coral canopy (thickness of 3.4 cm, fibre diameter 1 mm, and a porosity of 26%, as shown in Figure 3[1]). The third case was a rough surface with stones of the median diameter[2] of 3.28 (±0.38) cm that were glued in a square geometrical pattern over the entire surface of the acrylic panel, at an interval of 5 cm between each stone (see Figure 4), to represent large coral boulders (referred to by divers as "bummies", which sometimes can have diameters of several meters, with spacing of some metres between them[3]). Each of the experimental condition was tested for two different water depths, d_1 of 25 cm and 30 cm.

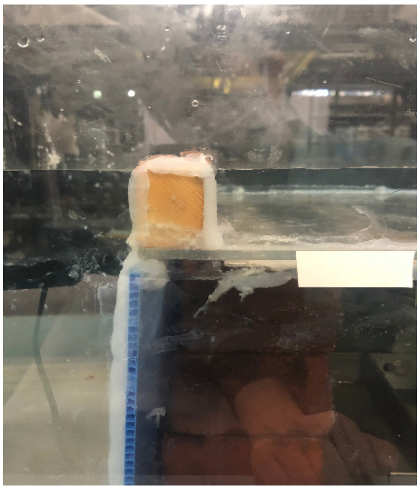

Figure 2: Appearance of reef edge in the wave flume

Figure 3: Appearance of polyethylene sheet in the wave flume

Figure 4: Appearance of stones installed in the wave flume

[1] The porosity of the branch tips of various *Acropora* species has been estimated to range from 33 to 70% (see Bucher et al., 1998).

[2] This was the median diameter of all the total sample of diameters for all the stones. Whenever any stones were elongated, the longest side of the stone was placed facing upwards (as this was thought to best represent how "bummies" exist in nature).

[3] Videos of the laboratory experiments, together with dives by one of the authors that show what some of these "bummies" look like can be see at https://www.youtube.com/watch?v=4MKkIo_O6cA&ab_channel=TsunamiFieldSurveys

Five wave gauges (WG) and two velocity metres (VM) were placed in the tank, as shown in Figure 1. All gauges employed (KENEK CHT6–30, 40) were of the capacitance type, with a range of 30 or 40 cm. The wave profile was measured using five wave gauges, one located in the middle of the tank, another before the reef edge, and the others on the reef flat (at the reef edge, halfway through the reef flat, at the end of reef flat, and on top of the metal false bed which represented the beach, see Figure 1).

The velocity meters (KENEK VMT2–200–04P, 04PL) employed in the experiment were all electromagnetic current metres (ECMs), with a range of measurement of 0.5 m/sec for VM1 and 1.0 m/sec for VM2. A low pass filter of 20 Hz was applied after the data acquisition. The VMs were placed just before the reef edge, 20 cm away from the bottom surface of the wave flume, and before the beach section (at the end of the reef flat section) at a height of 2.5 cm from the metal false bed, to attempt to measure the overtopping conditions. The velocity meters did not provide reliable results, and as thus the wave gauges were the main source of data for the experiments. Hence, the final analysis relied on wave-front tracking rather than the ECM measurements (as will be detailed later).

A video camera (CAM, SONY HDR-CX680, 60 fps) was used to record the behaviour of the wave as it broke over the reef edge. In addition, a GoPro HERO7 Black, which supports 4K/60 fps of video recording function was used to capture the solitary wave movement and observe its behaviour from the "beach". A PIV device was also installed (Kato Koken K8) although the results it provided (analyzed through the FlowExpert software) were inconclusive. This is to confirm the field reports by Shibayama et al. (2010) following the *2009 Samoan Tsunami*, which revealed that residents were able to observe wave breaking on the reefs and that this acted as a trigger to prompt them to evacuate.

The crest period (T_c), which represents the duration of significant water particle movement detected by movement of water surface, is shown in Table 1. As the experiments were carried out in a 1:100 scale, the T_c of each wave under field conditions are also shown in Table 1, which clearly shows that these would have been much lower than those of a typical tsunami wave (which can have periods of 10 minutes or longer, although at depths similar to those modelled in the present experiment the wave would have likely already steepened up, reducing its period, see Roubos et al., 2011). There were 4 different heights of waves generated for the experiment, with the input settings for each of them being 8 cm, 10cm, 12 cm, and 14 cm (which could correspond to 8 m, 10 m, 12 m, and 14 m in field, according to the scaling law used). Thus, in total there were 48 experimental conditions.

Table 1: Summary of inputted wave height, actual wave heights measured at WG1, and T_c of waves used in the experiments

Input wave height H_c (cm)	**Measured wave height at WG1 H_m (cm)**	**Water depth d_1 (cm)**	**T_c (sec)**	**T_c (in field) (sec)**
8	8.67	25	1.67	16.7
	8.85	30	2.01	20.1
10	10.86	25	1.52	15.2
	10.97	30	1.94	19.4
12	12.85	25	1.41	14.1
	13.20	30	1.68	16.8
14	14.98	25	1.38	13.8
	15.53	30	1.63	16.3

3 Results

3.1 Experiment repeatability

In the present study one of the experimental conditions was repeated 7 times for the case of smooth surface, d_I = 25 cm, l = 300 cm, and H_c = 14 cm. The results of this experiment, showing the maximum degree of variation above or below the mean, is shown in Table 2. WG3 for this experiment was an area of high turbulence, but otherwise the experimental errors for the other wave gauges were considered small enough that the other experimental conditions were only repeated 3 times (thus, while the overall trends observed in the experiments were pretty consistent, the quantitative differences between reef configurations should be interpreted as indicative rather than statistically definitive).

The measurements made by the velocity metres were much less consistent, as the data obtained from them was heavily affected by noise. Due to this, the present experiments could not improve on the methodology detailed in Esteban et al. (2017), and were thus omitted from the analysis.

Table 2: Standard deviation for one experiment condition.

Input wave height H_c (cm)	**Reef flat length l (cm)**	**Water depth d_I (cm)**	**Reef surface**	**WG1**	**WG2**	**WG3**	**WG4**	**WG5**
14	300	25	Smooth	0.01	0.02	0.11	0.04	0.07

3.2 Observation of solitary behaviour from the top of beach

The solitary wave behaviour recorded by the GoPro camera at the beach every 0.5 s is shown in Figure 5 for the conditions of d_I = 25 cm, H_c = 14 cm, l = 300 cm and a smooth surface. Other experimental conditions showed similar patterns, where the wave broke over the reef and became a bore, and which is similar to what was reported by Mikami to have happened during the *2009 Samoan Tsunami* (see Shibayama et al., 2010 and Mikami, 2015).

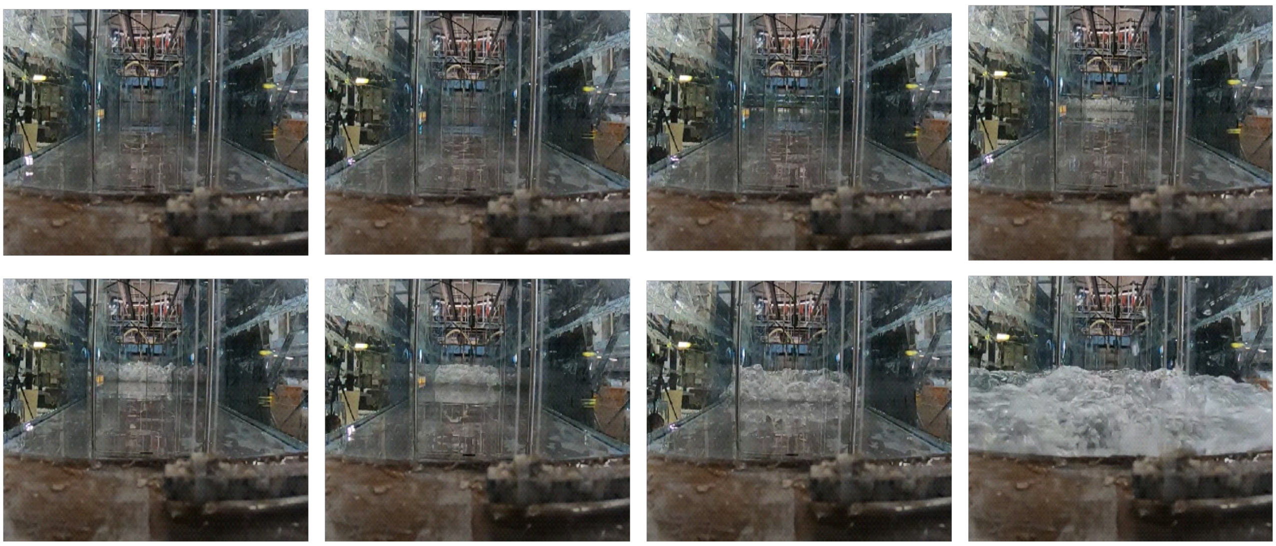

Figure 5: The screenshots of Go Pro video (Chronological order from top left to bottom right.)

3.3 Wave velocity

As stated earlier, it was challenging to obtain accurate readings from the velocity metres. In order to overcome this problem, the concept of wave front velocity was used to approximate the maximum kinetic energy present in the wave-like flow (following Dressler, 1954; Estrade and Martinot, 1964; and Chanson, 2006, who estimated that the flow velocity in a turbulent bore tip can be said to be roughly equal to the bore front velocity), although in the present work the concept of wave front velocity is used; i.e. the velocity of the particles at the very start of the wave, irrespective of whether it is a bore or solitary wave. The concept of wave front velocity is particularly important for the case of tsunami waves in disaster risk management, particularly for the case of the evacuation of residents (see Han et al., 2023, Takabatake et al., 2022).

Following Esteban et al. (2017), the wave front velocity was calculated according to the time for the bore tip to travel between WG1&2, 2&3, 3&4 and 4&5 (it should be noted that between WG1&2 and WG2&3 the wave could not be defined as a bore, but the same methodology was followed for consistency). The calculated data are given in Table A1 in the Appendix, and representative trends in the wave front velocity with distance are shown in Figure 6 (the remaining results are provided in Figures A1-3 in the Appendix).

It should be noted that, for a soliton propagating in deep water the wave celerity is typically much larger than the particle velocity. The soliton celerity can be approximated from theory using $c = \sqrt{gd_1}$, giving a range of 156 to 171 cm/s from the values in Table 1. This is similar, but not quite the same, as the values for the wave front velocity provided in Figure 6: Trends of wave front velocity in distance. Left, l = 300 cm, H_c = 12 cm. Right, l = 400 cm, H_c = 2 cm. Note that the reef crest is situated 550 cm from the wave generator (see Figure 1).

A comparison of the wave front velocity between WG1&2 and 3&4 is shown in Table 3. There is some difference in wave front velocity between WG1-2 between the experimental conditions, with difference of up to 8% in the case of stones being present. It should be noted that, while one might expect these values to be more homogeneous, in fact the wave motion at WG2 is already influenced by the characteristics of the reef behind it, explaining some of this variation. This is similar to what has been found in experiments with solitary waves and mud, where mud is seen to oscillate in the ground before the wave is on top of it (Soltanpour et al. 2019). However, it is also possible that the front shape of the solitary wave (as explained earlier, the front tip of the wave was used to calculate the wave front velocity) was less repeatable than the maximum wave height.

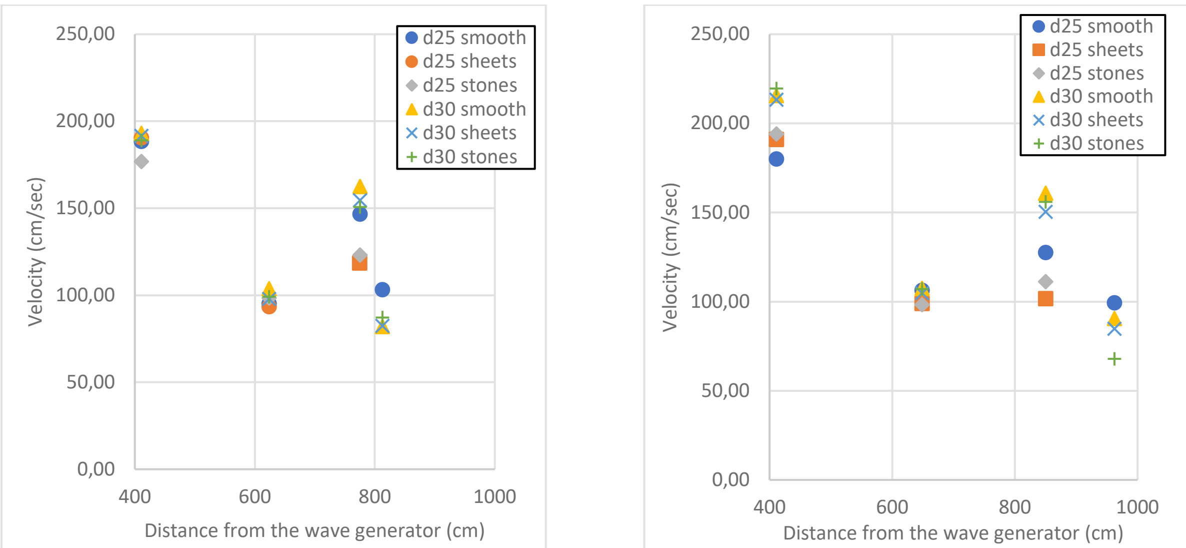

Figure 6: Trends of wave front velocity in distance. Left, l = 300 cm, H_c = 12 cm. Right, l = 400 cm, H_c = 2 cm. Note that the reef crest is situated 550 cm from the wave generator (see Figure 1).

Table 3: Ratio of the wave front velocity at the end of the reef flat compared to that at the beginning of the tank (expressed as the ratio of WG3~4/WG1~2)

Input wave height H_c (cm)	Water Depth d_1 (cm)	Reef surface	The ratio of wave front velocity (WG3~4/WG1~2) Reef length *l* (cm) 300	400
8	25	smooth	70.24%	61.10%
		sheets	46.61%	40.97%
		stones	58.87%	47.94%
	30	smooth	61.74%	76.44%
		sheets	62.00%	61.68%
		stones	57.84%	62.67%
10	25	smooth	71.28%	62.85%
		sheets	55.80%	47.78%
		stones	58.97%	53.19%
	30	smooth	72.01%	73.53%
		sheets	80.08%	63.75%
		stones	74.77%	68.33%
12	25	smooth	77.83%	70.86%
		sheets	62.20%	53.30%
		stones	69.58%	57.33%
	30	smooth	84.15%	74.59%
		sheets	80.65%	70.47%
		stones	79.73%	71.07%
14	25	smooth	68.13%	66.39%
		sheets	67.49%	56.33%
		stones	65.64%	56.20%
	30	smooth	83.87%	82.44%
		sheets	75.95%	71.50%
		stones	70.47%	75.18%

3.4 Results from wave gauges

As just indicated, given that there was some variability between experiments, all of the experimental conditions were repeated 3 times (Table A2 in the Appendix shows the average wave height at each of the WGs used. The average wave height recorded at WG1 was confirmed to be almost identical regardless of the reef surface (which thus confirmed that the wave heights are highly reproducible in the present experiments). However, the measurements at WG3 and WG4 showed more variation, which indicates that the generated wave is clearly affected by the reef structures.

Representative trends of the wave height over distance are shown in Figure 7 (with the remaining results given in Figures A4–A6 in the Appendix. Note also that figure A7 in the Appendix provides samples of the surface elevation timeseries). As explained earlier, the data shown in Table 1 and Figure 7 represent the average of each experimental case, which was conducted three times. Figure 7 shows that a clear reduction in wave height was observed after WG3 along the wave gauges placed over the reef flat, which indicates that the effect of the bottom friction deforms and slows down the wave.

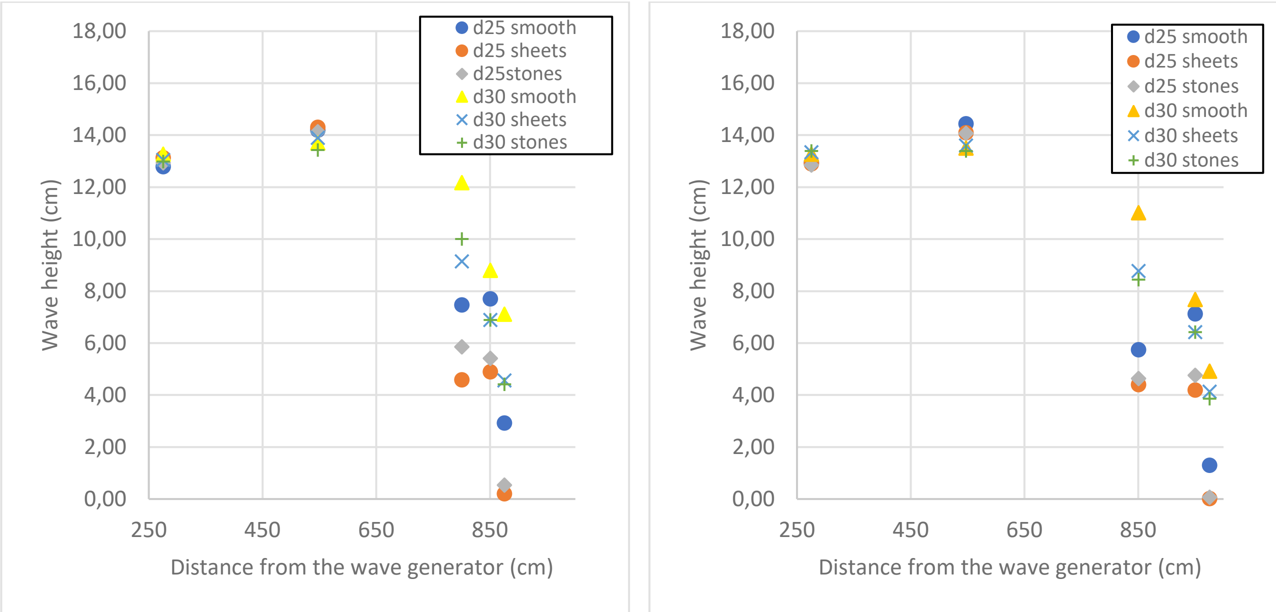

Figure 7: Trends of wave height with distance. Left, l = 300 cm, H_c = 12 cm. Right, l = 400 cm, H_c = 12cm.

Also, a comparison of the wave height at WG2 and WG4 is shown in Table 4 (Since the wave did not reach the top of the beach in some cases, WG5 was not included in this comparison). This shows that the reduction in wave height was greater with the existence of coral structures, with that due to the polyethylene sheets being greater than the stones. This indicates that different densities and roughness of corals affect the changes of wave height and velocity over the reef flat, given the differences between these structures (although it is important also to note that the porosity of structures is not the same, and that the precise magnitude of these differences should be interpreted with caution given the limited number of repetitions in each experimental condition). This trend was clearer with lower input wave heights. In addition to this, the trends were slightly different between different water depths, as in d_l = 25 cm, the wave heights tend to increase at WG4, whereas in d_l = 30 cm there was no increase at this point (probably partly due to the effect of the "beach" next to WG4).

Table 4: Comparison of wave height (note that values involving WG4 should be interpreted with caution as measurements at this location were affected by reflections from the beach section)

Input wave height H_c (cm)	Water depth d_1 (cm)	Reef surface	Wave height reduction (WG4/WG2) Reef Length l (cm) 300	Reef length l (cm) 400
8	25	smooth	40.49%	42.15%
		sheets	66.70%	72.88%
		stones	61.09%	62.03%
	30	smooth	22.44%	31.33%
		sheets	45.33%	45.04%
		stones	39.16%	39.92%
10	25	smooth	50.62%	45.29%
		sheets	67.88%	70.63%
		stones	60.81%	63.53%
	30	smooth	27.51%	34.58%
		sheets	45.38%	51.23%
		stones	44.89%	47.95%
12	25	smooth	45.73%	50.66%
		sheets	65.75%	70.22%
		stones	61.70%	66.21%
	30	smooth	35.84%	43.08%
		sheets	50.48%	52.80%
		stones	48.70%	52.05%
14	25	smooth	51.35%	54.02%
		sheets	65.66%	72.07%
		stones	64.27%	68.03%
	30	smooth	44.59%	49.61%
		sheets	56.85%	60.39%
		stones	54.07%	55.19%

4 Discussion

The experiments that were carried out confirmed that the existence of a reef flat structure results in a reduction in both wave heights and wave front velocity. This reduction was *generally* greater for the case of sheets (which would represent colonies of branching corals such as Elkhorn coral (*Acropora palmata*), then stones (representing "bummies", or colonies of boulder type corals such as the Blushing Star Coral (*Stephanocoenia intersepts*) and then a smooth surface (which would represent a bleached coral reef), similar to the experimental results by Buckley et al. (2016). Also, a longer reef flat and a shallower water depth led to reductions in both wave heights and bore front velocity. It is nevertheless important to note at this point that the use of the polyethylene sheets will result in large scale effects, and it is not clear how well these represent colonies of branching corals, which should be clarified in future research.

In terms of physics, the solitary wave propagates along the channel at almost constant velocity and encounters a sudden change in water depth (the coral reef). In the present case the reef crest, modelled with a wooden piece, which is typically shallower than the reef flat behind it (as conditions for coral growth are ideal in this area) had a significant influence on wave hydrodynamics, as what happens in reality. This will cause it to break and significantly lose velocity, leading to the formation of turbulence. This turbulence causes the formation of the bore. After the wave eventually transformed into fully developed bore –typically around WG3–, which has a higher velocity than during the wave breaking and bore formation phases (when wave breaking and turbulence dominate). Gradually, as the fully developed bore propagates over the channel it will lose energy due to turbulence and bottom friction (with the rougher bottom friction cases resulting in greater loses in velocity, as can be seen in Figure 6).

However, it should be noted that the measured data of wave heights at WG4 was somewhat imprecise, as it was greatly affected by the reflection from the beach structure, causing the wave gauges to measure higher values than at WG3. Although the waves were breaking and deforming at the reef edge (the wave was not bore at WG1 and WG2), the same methodology was applied to calculate the velocity at all points, and the changes in wave shape along the channel obviously indicate some of the shortcomings in calculating the wave velocity in such a manner.

It is also important to acknowledge that the bore-front tracking approach is subject to several sources of bias. The identification of the bore patterns relies on judgment on the side of the authors that were conducting this analysis, although as explained in Section 3.1., the results obtained across the various experiments were rather consistent. Nevertheless, these relied on an analysis of various frames at given time intervals, and there was some degree of variation between these for the same experimental condition (although all showed the same overall patterns).

When doing any experiments in the laboratory, it is important to ensure that the similitude laws used can accurate model a given problem. One parameter that can be used to gauge this is the notional Froude number *Fr* of the wave front, defined by equation (1),

$$Fr = \frac{V_i}{\sqrt{gH_i}} \tag{1}$$

where H_i is the actual wave height measured at a given wave gauge, and V_i is the wave front velocity (measured as the time taken for the wave to traverse the section between that preceding wave gauge and the point where H_i is measured). It is important to note that this *Fr* is not the steady flow Froude number, as it represents a bore propagating over a reef flat, and that the front velocity and (maximum) flow depth were not measured at the same time (and hence there is some uncertainty in the actual values). The *Fr* for the various types of reef flats (smooth, stones, or permeable sheets) was clearly different. In these experiments, the *Fr* ranged between1.50 and 2.23 at WG2, 0.84 and 1.61 at WG3, 1.37 and 1.98 at WG4 and 0.85 and 3.55 at WG5.

This *Fr* was calculated by using the wave front velocity and wave height measured at the wave gauge located at the beach side (e.g. for calculation of *Fr* at WG2, the wave front velocity between WG1&2 and wave height measured at WG2 are used). As such it is difficult to conclude that the *Fr* number was calculated accurately, especially given the issue of reflection at WG4 due to the beach structure (and thus the Fr numbers at this point should be treated with caution, and it should also be further noted that the definition of Fr number used here is not rigorous). Despite such shortcomings, it would appear that the numbers obtained are within the ranges of what can be considered realistic. Matsutomi et al. (2001) summarized *Fr* for past tsunami events, which they calculated using the surveyed flow depths and velocities estimated from Bernoulli's equation, and indicated that they ranged from 0.7 to 2.0 near the shoreline. Nevertheless, it is important to note that the present experiments do not accurately model tsunami waves, and should be viewed with caution. It is also important to acknowledge that, while Froude similarity is appropriate for reproduction the dominant influence of gravity in free-surface wave hydrodynamics, the effect of the bottom friction (particularly in complex flow experiments such as the ones here) is governed by Reynolds similarity, which was thus not appropriately modelled in the present experiments. Nevertheless, the present experiments essentially show that a solitary wave will steepen as it approaches the shore, and hence the relatively short period of the first half of the wave in the model – which determines to a large extent the initial attack by the wave – might be realistic for the 25 m depth that is modelled by the present experiments (see Roubos et al., 2021, who describe a surf-similarity parameter to predict tsunami characteristics at coast). In the numerical simulations, Kunkel et al. (2006) found that reefs are less effective against longer wavelength and larger amplitude tsunamis, particularly for shorter reef flats. Thus, the current experimental setup is likely to lead to an overestimation of the protection provided by the reef, particularly for tsunamis with longer wavelengths.

Given some of the shortcomings of these experiments, there are several areas of potential future research that could improve on the results. Firstly, there was some degree of variation within the measurements of the wave velocities at WG2. Experiments analysing the behaviour of mud layers to solitary waves note that there is an oscillation of the mud in the ground towards the shoreline of a solitary wave, prior to the arrival of the wave over it (with the gap between them probably being related to the height of the wave, and thus its wavelength, see Soltanpour et al. 2019). The precise effect that the reef structure has on the shape of the wave was not fully clarified by the present experiments, and although some patterns could be hypothesized, these need to be further clarified by further research. The experimental methodology for this would include more wave gauges being set between the paddle and the reef structure, and possibly pressure cells being placed around different parts of the reef edge and/or bottom of the channel. In this manner, the relationship between different wave parameters and reef layouts might be further clarified. However, it is also worth noting that part of the variation in the measurements of wave velocities at WG2 could also be due to fluctuations in the motor of the paddle (given that the machine was operated to the limit of its capacity) or other issues. While the fluctuations did not significantly influence the wave height of the solitary waves (in fact, wave heights were shown to be quite similar regardless of reef surface, see Table A1 in the Appendix), they might have influenced the front shape of the solitary wave (which was used to calculate the wave velocity). Despite such shortcomings, it is important to note that these do not detract from the overall conclusion of the paper, which clarified that the presence of reef flats helps to dissipate the energy of an incoming solitary wave, and that the protection offered increases with the length of this biological-legacy structure. This finding is directly relevant to the objectives set out in the introduction, namely to clarify how reef-flat characteristics influence the transformation of incoming solitary-wave-like disturbances as they propagate shoreward. Essentially, the experiments indicate that both the length of the reef-flat and the bottom roughness play an important role in modifying wave hydrodynamics after breaking over the reef edge, resulting in lower wave heights and reduced front velocities landward of the reef.

One important future task would be to try to improve on the measurement and calculation of the wave velocity. As discussed earlier, the same methodology of calculation was applied at WG1 and 2, although the waves were not bores at the point. In addition to this matter, the velocity meters were heavily effected by noise and were not able to obtain accurate results. Although PIV was used as an alternative way to measure velocity, the results were not perfect, given that a wide-angle was employed but neither the camera nor tracer used to capture the flow were well suited for it. In order to improve the accuracy of the measurement of the velocity, it would be preferable to use a tracer with larger particle sizes, if the PIV was to be taken over a larger area. It is also advisable to use non-white structures in the wave flume since the tracers tend to be white and the analytic system finds it hard to distinguish between structures and tracers. Secondly, it would be interesting to research a wider range of coral structures. The stones and polyethylene sheets aimed to represent different types and densities of corals species in this study, namely healthy coral reefs and smooth surfaces for bleached coral reefs. However, in nature there is a wide range in the density and the roughness of corals, and this could be one of the reasons explaining the various diverging theories regarding the influence of coral reefs on tsunami impact. Thus, the authors would like to suggest to investigate the effect of other degraded coral reef ecosystem (represented perhaps by a higher/lower density or by using smaller/larger stones) on solitary wave propagation over the reef flat. Finally, this study did not focus on differences in the characteristics of the reef slope or edge, which could have a significant effect on wave breaking, and which should be the target of future study.

It would also be interesting for future research to attempt to numerically reproduce the experiments that were conducted, which should first contemplate what is the most appropriate way of reproducing such complicated phenomena (i.e. either to use a Boussinesq-type model, non-hydrostatic wave-flow models or CFD models). This would allow for a more in-depth study of how the reef edge contributes to energy dissipation, and how the different roughness elements on the reef flat contribute to such processes. While numerical methods have their limitations, and can only demonstrate a general trend in wave behaviour, using the present experiments to validate them could then help the study of how real tsunami waves (which are somewhat different to those employed in the present experiments) interact with coral reefs.

5 Conclusions

In this study, the influence of coral reef analogues on solitary propagation over a reef flat was tested in a two-dimensional wave flume, focusing on the presence of corals and the length of the reef. The results confirm that the wave breaks over the reef and becomes a bore. Longer reefs, shallower water depth and the presence of coral analogues played a role in dissipating wave energy, lowering the wave height and its velocity. Essentially, as the waves break over the reef edge they then propagate over the reef flat as bores, which dissipate energy as they move toward the beach. While the findings clarify laboratory-scale hydrodynamic processes over reef-flat analogues, they should not be interpreted as direct tsunami-scale predictions, given the limitations in the methodology employed.

Hence, this study indicates that reef-flat analogues with greater roughness and longer lengths can enhance the attenuation of damage by solitary-wave-induced bores under the tested experimental conditions. As stated earlier, coral bleaching can result in mass coral mortality, which makes what is left of the skeletons of the corals smoother – i.e. a reduction in density or roughness due to erosion. Thus, this indicates that a solitary wave might have a greater impact in areas where bleaching is more pronounced, highlighting the increased risks that the warming of the seas due to climate change places on coastal settlements.

List of parameters

Parameter	Description
c	wave celerity
d_1	water depth before the reef
d_2	water depth over the reef flat
Fr	Froude number
g	acceleration of gravity
H_c	Input wave height
H_i	actual wave height measured at a given wave gauge
H_m	Measured wave height at WG1
h_r	height of the false metal bed above the bottom of the flume
l	Reef flat length
T_c	Crest period
V_i	wave front velocity

Acknowledgements

Funding

The work was partially supported by the Japan Society for the Promotion of Science (JSPS) KAKENHI Grant Number 20KK0107.

Author contributions (CRediT)

YN: Conceptualization, Data curation, Formal Analysis, Methodology, Laboratory Experiments, Validation, Visualization, Writing – original draft, Writing – review & editing. NI: Writing - review & editing, Investigation. TT: Writing – review & editing, Investigation, Supervision. ME: Methodology, Writing – original draft, Writing – review & editing, Supervision, Writing – final draft. TS: Investigation, Funding acquisition, Supervision.

Use of AI

No AI was used in this study.

Conflict of Interest (COI)

The authors report no conflict of interest.

References

Adger, W.N., Hughes T.P., Folke, C., Carpenter, S.R. and Rockström, J., (2005), Social-Ecological Resilience to Coastal Disasters, Science, 309(5737), 1036–1039.

Ahrens, J., 1987, Characteristics of Reef Breakwaters, USAE CERC TR 87-17, Vicksburg.Alongi, D.M., (2008), Mangrove forests: Resilience, protection from tsunamis, and responses to global climate change, Estuarine, Coastal and Shelf Science, 76(1), 1–13.

Baird, A.H., Campbell, S.J., Anggoro, A.J., Ardiwijaya, R.L., Fadli, N., Herdiana, Y., Kartawijaya, T., Mahyiddin, D., Mukminin, A., Pardede, S.T., Pratchett, M.S., Rudi, E. and Siregar, A.M., (2005), Acehnese Reefs in the Wake of the Asian Tsunami, Current Biology, 15(21), 1926–1930.

Bucher, D. J., Harriott, V. J. and Roberts, L. G. (1998) Skeletal micro-density, porosity and bulk density of acroporid corals, Journal of Experimental Marine Biology and Ecology, 228, 117–136.

Buckley, M.L., Lowe R.J., Hansen, J.E. and Dongeren, A.P., (2016), Wave Setup over a Fringing Reef with Large Bottom Roughness, Journal of Physical Oceanography, 46(8), 2317–2333.

Buckley, M.L., Lowe, R.J., Hansen, J.E., van Dongeren, A.R., and Storlazzi, C.D., (2018), Mechanisms of Wave-Driven Water Level Variability on Reef-Fringed Coastlines, Journal of Geophysical Research: Oceans, 123(5), 3811–3831.

Buckley, M. L., Lowe, R. J., Hansen, J. E., van Dongeren, A. R., Pomeroy, A., Storlazzi, C. D., et al. (2022). Wave-driven hydrodynamic processes over fringing reefs with varying slopes, depths, and roughness: Implications for coastal protection. Journal of Geophysical Research: Oceans, 127, e2022JC018857.

Burke L, Reytar K, Spalding M, and Perry A, (2011) Reefs at risk revisited. World Resources Institute. http://www.wri.org/. Accessed 13 May 2012

Chanson, H., (2006) Analytical solutions of laminar and turbulent dam break wave, in R.M.L. Ferreira, E.C.T.L. Alves, J.G.A.B. Leal, and A.H. Cardoso eds. Proc. Int. Conf. Fluvial Hydraulics River Flow 2006, Vol. 1: Taylor & Francis Groupe, London, pp. 465–474. (ISBN:0-415-40815-6).

Chatenoux, B., Peduzzi, P., (2007), Impacts from the 2004 Indian Ocean Tsunami: analysing the potential protecting role of environmental features. Nat Hazards, 40, 289–304.

Cochard, R., Ranamukhaarachchi, S.L., Shivakoti, G.P., Shipin, O.V., Edwards, P.J. and Seeland, K.T, (2008), The 2004 tsunami in Aceh and Southern Thailand: A review on coastal ecosystems, wave hazards and vulnerability, Perspectives in Plant Ecology, Evolution and Systematics, 10(1), 3–40.

Den Bieman, J., de Ridder, M., and Doeleman, M. (2024). Validation of an efficient two-layer non-hydrostatic wave model on a sloping foreshore. Journal of Coastal and Hydraulic Structures, 4. https://doi.org/10.59490/jchs.2024.0038

Dressler, R. F., (1954), Comparison of theories and experiments for hydraulic dam-break wave. Int. Assoc. Sci. Pubs, Vol. 38, No. 3, pp. 319–328.

Esteban, M., Glasbergen, T., Takabatake, T., Hofland, B., Nishizaki, S., Nishida, Y., Stolle, J., Nistor, I., Bricker, J., Takagi, H. and Shibayama, T. (2017) Overtopping of Coastal Structures by Tsunami Waves. Geosciences, 7(4), 121. [doi:10.3390/geosciences7040121]

Esteban, M., Roubos, J.J., Iimura, K., Salet, J.T., Hofland, B., Bricker, J., Ishii, H., Hamano, G., Takabatake, T. and Shibayama, T., (2019), Effect of bed roughness on tsunami bore propagation and overtopping, Coastal Engineering, 157-103539.

Esteban, M., Takabatake, T., Achiari, H., Mikami, T., Nakamura, R., Gelfi, M., Panalaran, S., Nishida, Y., Inagaki, N., Chadwick, C., Oizumi, K. and Shibayama, T. (2021) Field survey of flank collapse and run-up heights due to the 2018 Anak Krakatau Tsunami, Journal of Coastal and Hydraulic Structures, 1 (1).

Estrade, J., and Martinot, A., (1964). Ecoulment consecutif a la suppression dun barrage dans un canal horizontal de section rectangulaire, Comptes Rendus Hebdomadaires des Seances de L'Acadmie Des Sciences, 259(25), 4502 (in french).

Fernando, H.J.S., Samarawickrama, S.P., Balasubramanian, S., Hettiarachchi, S.S.L. and Voropayeva, S., (2008), Effects of porous barriers such as coral reefs on coastal wave propagation, Journal of Hydro-environment Research, 1(3-4), 187–194.

Fernando, H.J.S., McCulley, J.L., Mendis, S.G. and Perera, K., (2011), Coral poaching worsens tsunami destruction in Sri Lanka, Transactions American Geophysical Union, 86(33), 301–304.

Gelfenbaum, G., Apotsos, A., Stevens, A.W. and Jaffe, B., (2011), Effects of fringing reefs on tsunami inundation: American Samoa, Earth-Science Reviews, 107 (1-2), 12–22.

Han, D.C., Takabatake, T., Esteban, M., and Shibayama, T. (2023) Development and implementation of a smartphone application to support tsunami evacuation, International Journal of Disaster Risk Reduction, 96, 103915, https://doi.org/10.1016/j.ijdrr.2023.103915

Hanson, H. and Kraus, N.C., 1989. GENESIS: Generalised model for simulating shoreline change. Report 1: Technical Reference, Tech. Rep. CERC-89-19, US Army Engr., WES, Vicksburg, MS.

Hofland, B., Houtzager, D., Caldera, G., Antonini, A., van Gent, M. ., Bakker, P., and van der Lem, C. (2023). Rocking of single-layer armour units measured by embedded sensors. Journal of Coastal and Hydraulic Structures, 3. https://doi.org/10.59490/jchs.2023.0028

Kathiresan, K., Rajendran, N., (2005), Coastal mangrove forests mitigated tsunami, Estuarine, Coastal and Shelf Science, 65(3), 601–606.

Kunkel, C.M., Hallberg, R.W., Oppenheimer, M., (2006), Coral reefs reduce tsunami impact in model simulations, Geophysical Research Letters, 33(23).

Koyano, K., Takabatake, T., Esteban, M. and Shibayama, T. (2022) Magnification of tsunami risks due to sea level rise along the eastern coastline of Japan, Journal of Coastal and Hydraulic Structures, https://doi.org/10.48438/jchs.2022.00012

Loy Rego (2021), Social and Economic Impact of December 2004 Tsunami, Asian Disaster Preparedness Centre, 24 Oct 2021.

Lowe, R. J., Falter, J. L., Bandet, M. D., Pawlak, G., Atkinson, M. J., Monismith, S. G., and Koseft, J. R. (2005) Spectral wave dissipation over a barrier reef. Journal of Geophysical Research, 110, doi: 10.1029/2004JC002711.

Lowe, R.J., Falter, J. L., Koseff, J. R., Monismith, S. G., and Atkinson, M. J. (2007) Spectral wave flow attenuation with submerged canopies: Implications for wave energy dissipation. Journal of Geophysical Research, 112, doi: 10.1029/2006JC003605.

Majumdar, D., Chakraborty, S., Saha, S. and Datta, D., (2019), Geospatial analysis of the effects of tsunami on coral and mangrove ecosystems of Mayabunder in Andaman Islands, India, Braz. j. oceanogr, 67.

Matsuba, S., (2015), Analysis of tsunami behavior and effect of coastal forest in reducing tsunami force around coastal dikes, pp 46–50.

Matsutomi, H., Shuto, N., Imamura, F. and Takahashi, T., (2001) Filed Survey of the 1996 Irian Jaya Earthquake Tsunami in Biak Island, Natural Hazards, 24(3), pp. 199–212.

Mikami, T. (2015) Tsunami Disasters in Remote Islands: 2009 Samoan and 2010 Mentawai Island Tsunamis. In Handbook of Coastal Disaster Mitigation for Engineers and Planners. Esteban, M., Takagi, H. and Shibayama, T. (eds.). Butterworth-Heinemann (Elsevier), Oxford, UK.

Mikami, T., Shibayama, T., (2012), Numerical analysis of tsunami propagating on wide reef platform using turbulence model, JSCE B2, 68(2), I_076-I_080.

National Oceanic and Atmospheric Administration, (2021) What is coral bleaching?, National Ocean Service website, 24 Oct 2021.

Quataert, E., Storlazzi, C., van Rooijen, A., Cheriton, O., and van Dongeren, A., (2015), The influence of coral reefs and climate change on wave-driven flooding of tropical coastlines, Geophysical Research Letters, 42(15), 6497-6415.

Quironga, P. D. and Cheung, K. F. (2013) Laboratory study of solitary-wave transformation over bed-form roughness on fringing reefs. Coastal Engineering 80, 35–48.

Roubos, J., Glasbergen, T., Hofland, B., Bricker, J. D., Zijlema, M., Esteban, M. and Tissier, M. F. S. (2021) Formulation of a surf-similarity parameter to predict tsunami characteristics at the coast, Journal of Coastal and Hydraulic Structures, 1, DOI: https://doi.org/10.48438/jchs.2021.0009

Ross, R., (2018), What Are Coral Reefs?, Live Science, Oct 24 2021.

Seabrook, S.R. and Hall, K.R., 1998, Wave transmission at submerged rubble mound breakwaters, 26th Int. Conf. On Coastal Eng., Copenhagen.

Seemann, A., Melling, G., Jansch, H., and Kondziella, B. (2023). A design method for rock groynes exposed to overtopping from long-period ship wave loads. Journal of Coastal and Hydraulic Structures, 3. https://doi.org/10.59490/jchs.2023.0029

Sekimoto, T., Nakajima, S., Katayama, H. and Takahashi, K., (2011), Wave breaking on the reef with steep forereef slope and wave deformation model based on energy balance equation, JSCE B2, 67(2), I_011-I_015.

Shibayama, T., Mikami, T., Matsumaru, R., Takagi, H. and Latu, F., (2010), Field Survey and Analysis of Tsunami Disaster in the Samoan Islands, JSCE B2, 66(1), 1376–1380.

Shibayama, T. (2015) 2004 Indian Ocean Tsunami. In Handbook of Coastal Disaster Mitigation for Engineers and Planners. Esteban, M., Takagi, H. and Shibayama, T. (eds.). Butterworth-Heinemann (Elsevier), Oxford, UK.

Soltanpour, M., Shamsnia, S. H., Shibayama, T. and Nakamura, R. (2019) Experimental and analytical investigation of the response of a mud layer to solitary waves. Ocean Dynamics 70, 165–186.

Sorgatz, J., van den Eijnden, A. P., Montenegro, H., and Hicks, M. A. (2023). On the design of bank revetments at inland waterways subjected to ship-induced water level drawdown: A probabilistic infinite slope analysis. Journal of Coastal and Hydraulic Structures, 3. https://doi.org/10.48438/jchs.2023.0024

Takabatake, T., Esteban, M. and Shibayama, T. (2022) Simulated effectiveness of coastal forests on reduction in loss of lives from a tsunami, International Journal of Coastal Risk Reduction, 74, 102954, https://doi.org/10.1016/j.ijdrr.2022.102954

Tanaka, N., Sasaki, Y., Mowjood, M.I.M., Jinadasa, K.B.S.N. and Homchuen, S., (2006), Coastal vegetation structures and their functions in tsunami protection: experience of the recent Indian Ocean tsunami, Landscape Ecol Eng, 3, 33–45.

Van der Meer, J.W., 1990a. Low-crested and reef breakwaters. Delft Hydraulics Report H 986.

Van der Meer, J. W., Lykke Andersen, T., and Roge Eldrup, M. (2024). Rock Armour Slope Stability under Wave Attack in Shallow Water. Journal of Coastal and Hydraulic Structures, 4. https://doi.org/10.59490/jchs.2024.0035

Van Gent, M. R. (2024). Submerged low-crested structures in front of coastal structures. Journal of Coastal and Hydraulic Structures, 4. https://doi.org/10.59490/jchs.2024.0033

Villanoy, C., David, L., Cabrera, O., Atrigenio, M., Siringan, F., Aliño, P. and Villaluz, M., (2012), Coral reef ecosystems protect shore from high-energy waves under climate change scenarios, Climatic Change, 112, 493–505.

Watanabe, S., (2017), Mechanism of tsunami reduction effects of Teizan-canal, pp 43.

Yao, Y., Jia, M., Jiang, C., Zhang, Q. and Tang, Z., (2020), Laboratory study of wave processes over fringing reefs with a reef-flat excavation pit, Coastal Engineering, 158, 103700.

Yamamoto, L. and Esteban, M. (2014) Atoll Island States and International Law – Influence of Climate Change on Sovereignty and Human Rights, Springer, New York, ISBN 978-3-642-38186-7

The Editors of Encyclopaedia Britannica, Coral Reef, Britannica, 24 Oct 2021.

Appendix A

A1. Trends in wave front velocity with distance

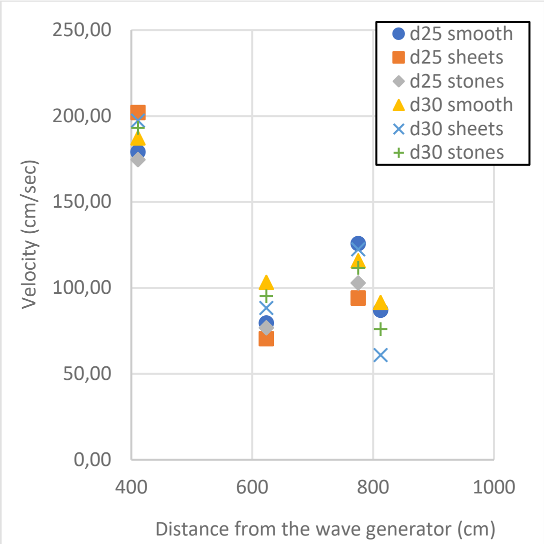

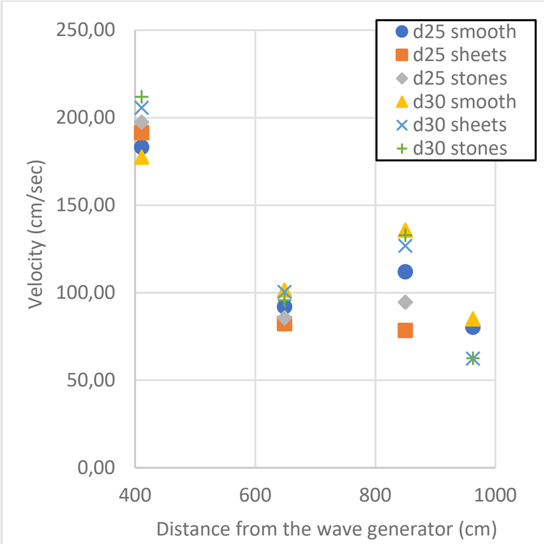

Figure A1: Trends of wave front velocity with distance. Left, $l = 300$ cm, $H_c = 8$ cm. Right, $l = 400$ cm, $H_c = 8$ cm.

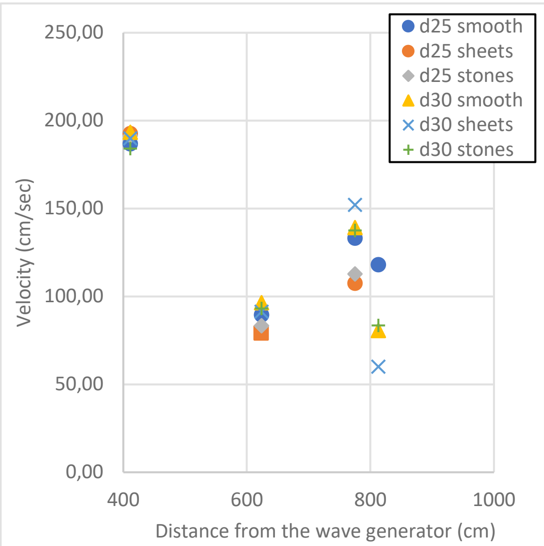

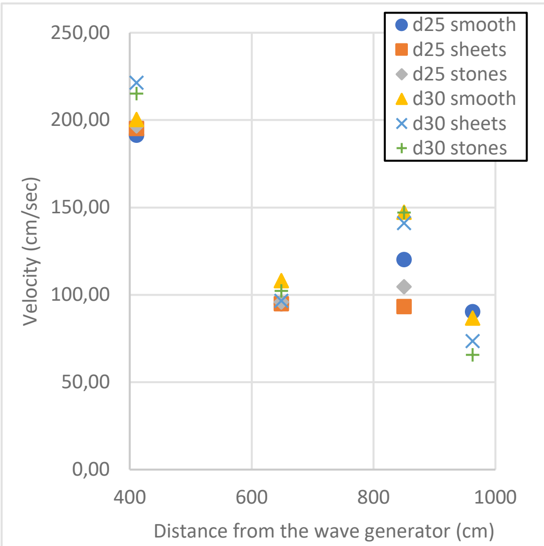

Figure A2. Trends of wave front velocity with distance. Left, $l = 300$ cm, $H_c = 10$ cm. Right, $l = 400$ cm, $H_c = 10$ cm.

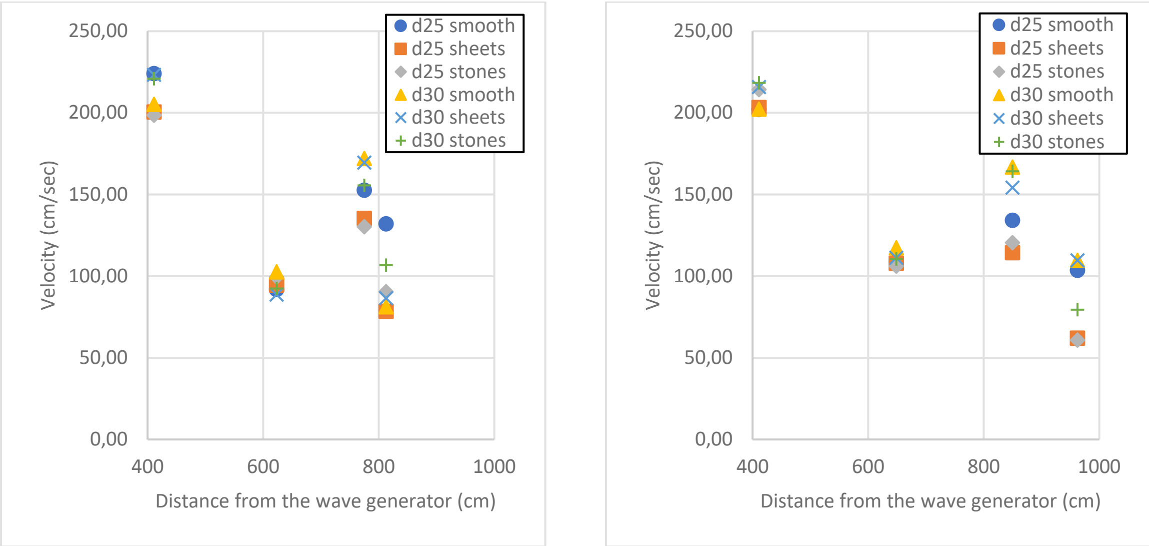

Figure A3:8 Trends of wave front velocity with distance. Left, l = 300 cm, H_c = 14 cm. Right, l = 400 cm, H_c = 14 cm.

Table A1: Results of wave front velocity. In some cases the wave did not overtop the beach, and thus WG4-5 is given as N/D.

Reef flat length l (cm)	Input wave height H_c (cm)	Water Depth d_1 (cm)	Reef surface	WG1~2 (cm/sec)	WG2~3 (cm/sec)	WG3~4 (cm/sec)	WG4~5 (cm/sec)
300	8	25	smooth	178.99	79.45	125.72	86.95
			sheets	201.90	70.32	94.11	N/D
			stones	174.57	76.71	102.77	N/D
		30	smooth	187.20	103.17	115.58	91.49
			sheets	197.27	88.22	122.30	60.95
			stones	192.98	95.09	111.61	75.89
	10	25	smooth	186.95	89.65	133.25	118.21
			sheets	192.71	79.06	107.53	N/D
			stones	191.52	83.47	112.93	16.37
		30	smooth	193.39	96.60	139.26	80.77
			sheets	190.02	91.37	152.16	60.14
			stones	184.16	93.23	137.71	83.62
	12	25	smooth	188.51	95.14	146.71	103.33
			sheets	190.49	93.58	118.49	N/D
			stones	176.97	98.43	123.14	N/D
		30	smooth	193.10	103.73	162.50	82.15
			sheets	191.69	97.98	154.60	82.40
			stones	189.09	99.15	150.76	87.14
	14	25	smooth	224.08	91.78	152.66	131.99
			sheets	200.54	94.45	135.34	78.39
			stones	198.45	99.47	130.26	90.39
		30	smooth	205.20	102.60	172.09	81.26
			sheets	223.18	88.73	169.50	86.56
			stones	220.79	92.47	155.59	106.79
400	8	25	smooth	183.05	91.98	111.84	80.25
			sheets	191.31	82.29	78.37	N/D
			stones	197.28	85.49	94.57	N/D
		30	smooth	177.39	101.48	135.61	84.96
			sheets	205.58	100.38	126.80	62.26
			stones	211.82	95.69	132.75	62.55
	10	25	smooth	191.50	95.02	120.36	90.39
			sheets	195.28	95.10	93.31	N/D
			stones	196.87	96.03	104.72	N/D
		30	smooth	200.46	108.24	147.41	86.82
			sheets	221.47	96.68	141.18	73.66
			stones	215.27	102.28	147.10	65.84
	12	25	smooth	180.17	106.39	127.67	99.37
			sheets	191.00	99.05	101.79	N/D
			stones	194.18	98.31	111.33	N/D
		30	smooth	215.58	107.51	160.80	90.56
			sheets	213.39	104.79	150.37	84.89
			stones	219.57	107.10	156.06	67.93
	14	25	smooth	202.11	109.11	134.19	103.52
			sheets	203.12	107.90	114.41	61.99
			stones	214.19	106.10	120.37	60.83
		30	smooth	202.22	117.31	166.70	109.64
			sheets	215.74	111.26	154.25	109.71
			stones	218.38	110.44	164.18	79.41

A2. Trends of wave height with distance

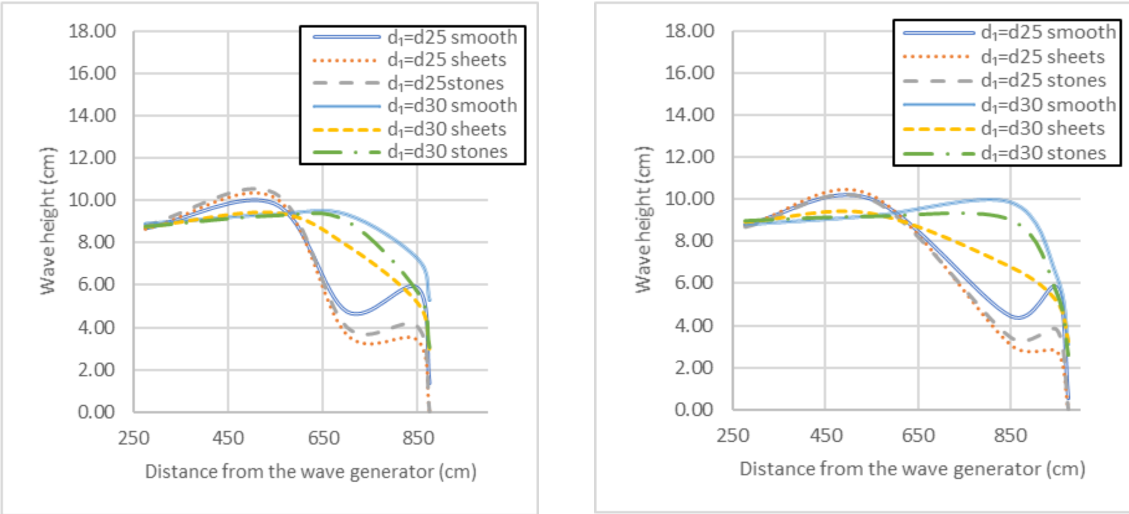

Figure A4: Trends of wave height with distance. Left, l =300 cm, Hc = 8 cm. Right, l = 400 cm, Hc = 8 cm.

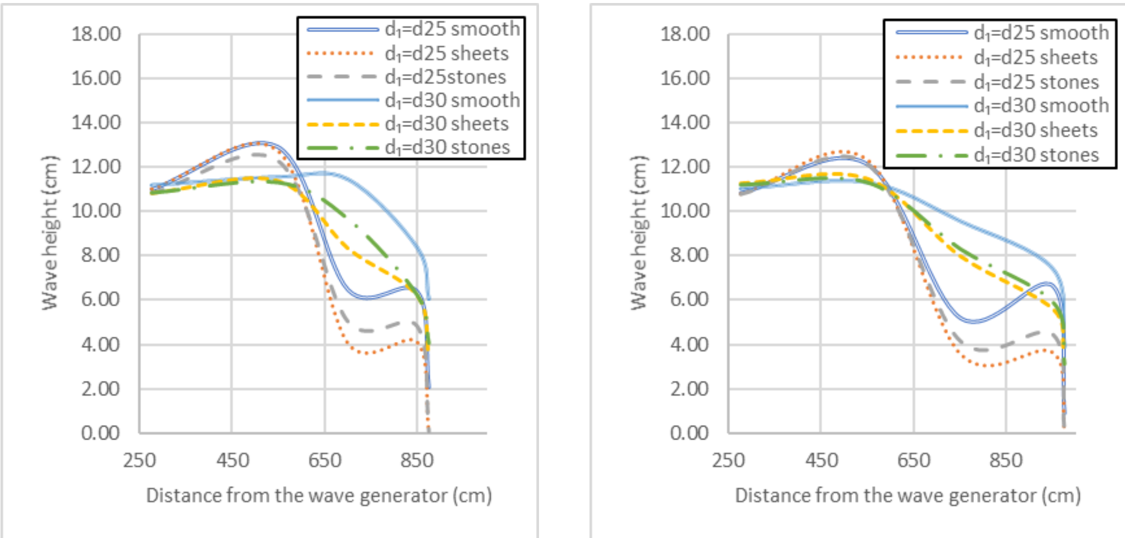

Figure A5: Trends of wave height with distance. Left, l = 300 cm, H_c = 10 cm. Right, l = 400 cm, H_c = 10 cm.

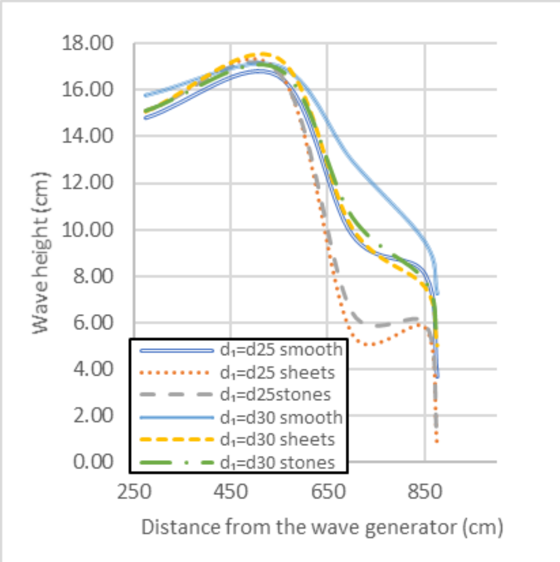

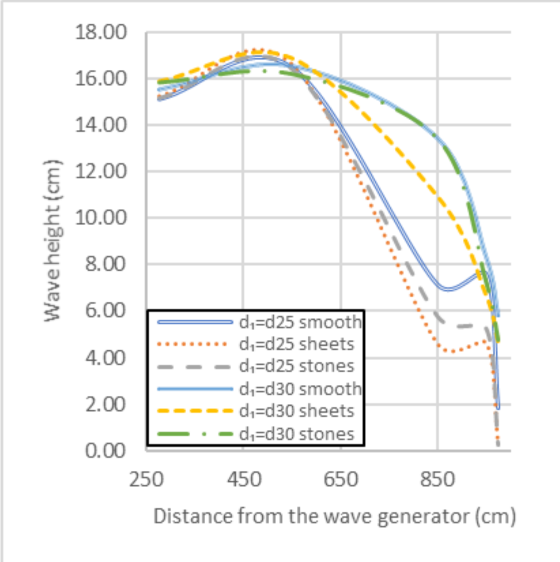

Figure A6: Trends of wave height with distance. Left, l = 300 cm, H_c = 14 cm. Right, l = 400 cm, H_c = 14 cm.

Table A2: Summary of experimental conditions and results

Input Wave height H_c (cm)	Reef flat length l (cm)	Water depth d_1 (cm)	Reef surface	WG1 (cm)	WG2 (cm)	WG3 (cm)	WG4 (cm)	WG5 (cm)	VM1 (cm/sec)	VM2 (cm/sec)
8	300	25	smooth	8.69	9.87	4.76	5.87	1.36	11.17	30.73
			sheets	8.65	10.15	3.65	3.38	0.00	17.94	16.47
			stones	8.81	10.36	4.02	4.03	0.01	10.84	20.70
		30	smooth	8.92	9.37	9.36	7.27	5.32	11.94	32.58
			sheets	8.74	9.43	7.88	5.15	2.94	6.38	19.99
			stones	8.78	9.30	9.04	5.66	3.05	9.21	27.02
	400	25	smooth	8.78	10.00	4.43	5.79	0.52	14.98	29.87
			sheets	8.72	10.19	3.06	2.76	0.00	8.05	9.31
			stones	8.71	10.02	3.44	3.80	0.00	15.19	9.41
		30	smooth	8.80	9.20	9.85	6.32	3.10	15.96	30.13
			sheets	8.93	9.35	6.78	5.14	3.22	16.99	12.47
			stones	9.00	9.21	9.04	5.53	2.57	13.79	22.44
10	300	25	smooth	10.98	12.91	6.46	6.38	2.06	10.22	26.14
			sheets	11.01	12.74	4.04	4.09	0.00	22.10	17.97
			stones	10.84	12.32	5.04	4.83	0.07	12.24	21.42
		30	smooth	11.19	11.56	11.45	8.38	6.07	12.50	36.75
			sheets	10.82	11.37	8.33	6.21	3.49	7.94	22.82
			stones	10.82	11.29	9.65	6.22	4.08	10.16	30.27
	400	25	smooth	10.82	12.14	5.20	6.64	0.92	15.94	32.33
			sheets	10.81	12.37	3.56	3.63	0.01	9.05	9.28
			stones	10.78	12.16	4.13	4.43	0.00	17.27	10.17
		30	smooth	11.06	11.35	9.58	7.42	3.90	18.25	34.68
			sheets	11.29	11.50	7.99	5.61	3.64	15.51	13.31
			stones	11.19	11.31	8.29	5.89	3.10	15.81	22.82
12	300	25	smooth	12.78	14.19	7.47	7.70	2.92	12.24	26.43
			sheets	13.13	14.30	4.59	4.90	0.20	10.32	18.75
			stones	12.94	14.13	5.85	5.41	0.54	13.18	27.34
		30	smooth	13.26	13.70	12.16	8.79	7.11	15.49	42.84
			sheets	13.05	13.89	9.14	6.88	4.56	10.03	22.43
			stones	12.98	13.42	10.00	6.89	4.41	10.68	37.89
	400	25	smooth	12.94	14.44	5.74	7.12	1.29	19.14	30.52
			sheets	12.90	14.08	4.40	4.19	0.02	10.02	10.19
			stones	12.84	14.07	4.63	4.75	0.06	18.97	11.57
		30	smooth	13.26	13.49	11.02	7.68	4.91	19.39	36.59
			sheets	13.34	13.59	8.77	6.42	4.13	18.15	12.44
			stones	13.38	13.39	8.44	6.42	3.85	16.83	22.30
14	300	25	smooth	14.79	16.60	9.77	8.08	3.68	11.23	32.78
			sheets	15.09	16.86	5.49	5.79	0.60	9.31	19.66
			stones	15.13	16.78	6.44	6.00	0.93	15.62	27.57
		30	smooth	15.76	17.03	12.94	9.44	7.22	14.26	42.04
			sheets	15.08	17.38	10.05	7.50	4.99	9.41	27.51
			stones	15.13	16.95	10.54	7.79	5.17	12.01	45.93
	400	25	smooth	15.09	16.49	7.12	7.58	1.81	22.35	37.87
			sheets	15.27	16.67	4.59	4.66	0.25	10.76	10.97
			stones	15.14	16.43	5.75	5.25	0.23	23.80	13.09
		30	smooth	15.54	16.56	13.44	8.34	5.83	15.05	39.50
			sheets	15.87	16.88	10.92	6.69	4.65	14.36	20.82
			stones	15.83	16.20	13.41	7.26	4.75	18.13	25.11

A3. Surface elevation timeseries

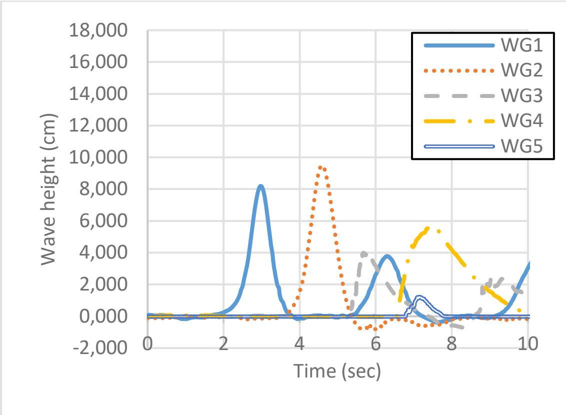

d_1 = 25 cm, smooth surface

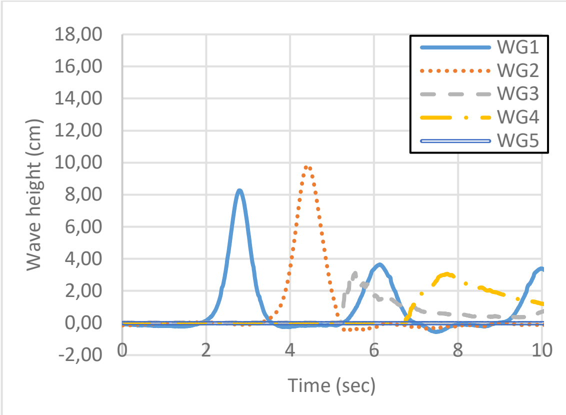

d_1 = 25 cm, with polyethylene sheet

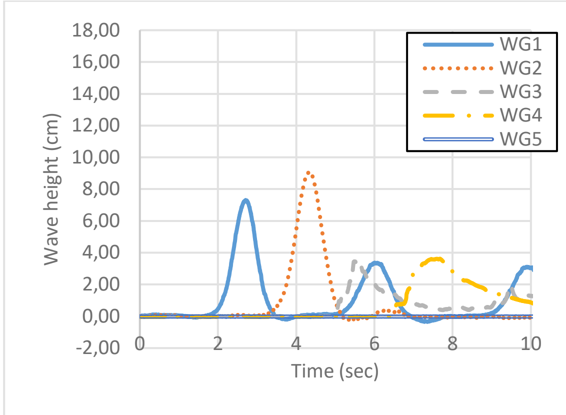

d_1 = 25 cm, with stones

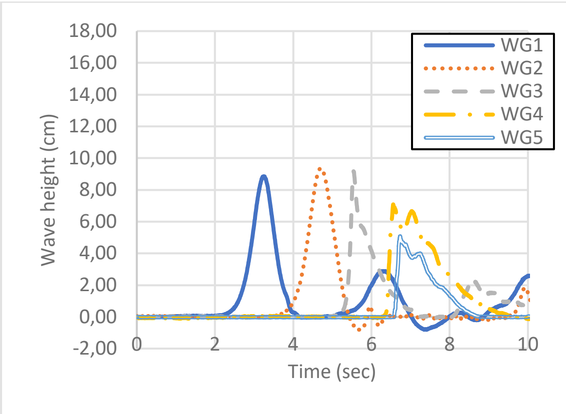

d_1 = 30 cm, smooth surface

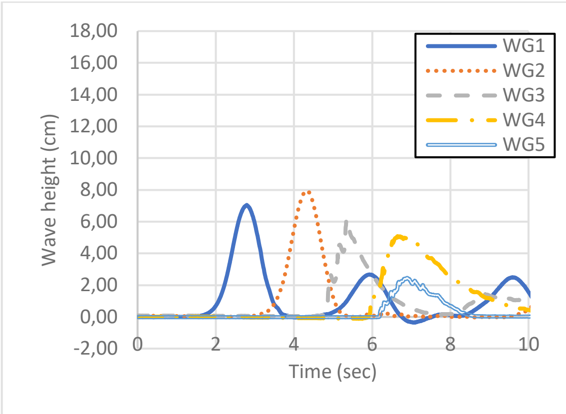

d_1 = 30 cm, with polyethylene sheet

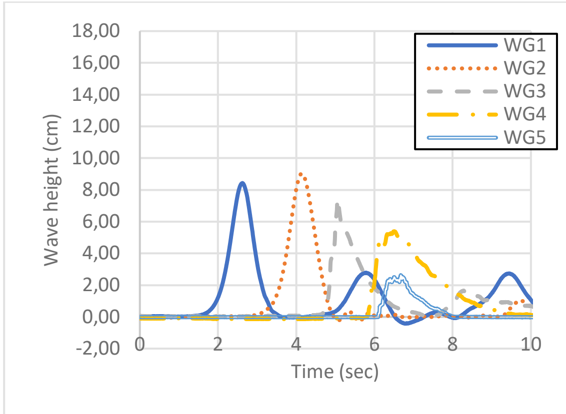

d_1 = 30 cm, with stones

Figure A7: Trends of wave height with time (l = 300 cm, h = 8 cm).